OPTICAL FIBER TECHNOLOGY **2**, 98-105 (1996)
ARTICLE NO.0011

Elimination of Optical Fiber Breaks in Stainless Steel Packages for $LinbO_3$ Optical Modulator Devices

HIROTOSHI NAGATA, NAOKI MITSUGI, MASARU SHIROISHI, TSUTOMU SAITO, TAKASHI TATEYAMA, AND SUSUMU MURATA

Optoelectronics Division of the Central Research Laboratories, Sumitomo Osaka Cement Co.,Ltd., Toyotomi-cho 585, Funabashi-shi, Chiba 274, Japan

Received June 1, 1995

Mechanical reliability of optical fibers fed to a stainless steel (AISI 303) package was investigated to achieve a hermetically sealed $LiNbO_3$ modulator device for optical communication systems. The fiber jacketed with an ultraviolet radiation-cured resin (acrylate) and a hytrel loose tube was sealed to ensure high mechanical stability during temperature fluctuations. The sealing of the fibers was completed using a soldering technique. The assembled devices were exposed under mechanical tests of Bellcore's TR-NWT-000468 requirement, and no deterioration was observed in the installed fibers. The proposed package structure can achieve a fiber-break-free $LiNbO_3$ device.

1. INTRODUCTION

Fiber breaks in optical devices have been discussed frequently from the viewpoint of reliability and estimated lifetime for optical communication systems [1-8]. Compared to the improvement in manufacturing of reliable long-haul fibers, however, a reliable procedure for joining fiber to the devices has not been developed and must be further investigated [9-17]. Concerning this problem, many failure models have been proposed for fiber breaks occurring in packaged passive devices [18]. The origin of most breaks in the exposed fibers is reported to be surface flaws which are possibly induced by fiber jacket removal processes with improperly designed jacket cutters [19, 20]. Fortunately, such failed fibers can be rejected by proof tests such as a bending test [16, 21]. Further, undesirable fiber buckling in the ferrule (or fiber feedthrough pipe) has been strongly indicated as a reason for the fiber breaks [3, 22].

This article discusses fiber breaks due to the fiber buckling phenomenon in order to obtain highly reliable *z*-cut $LiNbO_3$ (LN) devices. The LN devices, such as Mach-Zehnder optical intensity modulators and polarization scramblers, have been considered as promising devices to achieve high-speed optical communication systems [23]. The devices must be hermetically sealed to ensure stable operation over a period of 15-20 years. For such purposes, Kovar metal is commonly used for the package because its lower thermal expansion is close to that of device materials [24]. However, the thermal expansion of LN crystals is 30 times greater than the Kovar metal, and stainless steel is more suitable as the package material in this regard. The thermal expansions of LN (normal to the *z*-axis) and stainless steel (AISI 303) were measured and they matched very well throughout more than 200 K of temperature change [25]. A mismatch in thermal expansion leads to temperature dependent fluctuations in output signals of the device via the piezo-optical effect of the LN, so a stainless steel package must be applied to the LN devices. However, a larger thermal expansion of the package has disadvantages for the assembled optical fibers, namely fiber breaks due to a large mismatch of the thermal expansion. Here, the fiber feedthrough structure of the stainless steel package for the LN modulator devices was studied from the viewpoint of its mechanical stability. The mechanical tests from Bellcore's TR-NWT-000468 requirement were carried out on the fabricated samples, and no failures such as fiber breaks were observed.

2. MODULATOR PACKAGE FIBER FEEDTHROUGH STRUCTURE

Figure 1a shows a schematic illustration of the fiber feedthrough of the package. The package size is 120 mm × 15 mm × 10 mm, while the LN device chip was 60 mm × 0.8 mm × 0.5 mm. The package was made of stainless steel AISI 303. In the fiber assembly process, at first the optical fiber was inserted into a brass tube, as shown in Fig. 1b, and bonded to the tube using a thermally curable epoxy adhesive material (E, EpoTek 353 ND). The length, outer diameter, and inner diameter of the brass tube were 6.0, 1.4, and 0.45, respectively. The purpose of this tubing was to immobilize the end of the fiber jackets because, during the jacket removal process, possibly the bonding between the glass fiber and the jacket was broken near the removed point. In some fibers, a slight gap was observed at the glass/jacket interface after the jacket removal process [26]. A fiber coated with an ultraviolet radiation curable resin (acrylate) with a diameter of 400 μm was used here (hereafter de-

1068-5200/96 $18.00

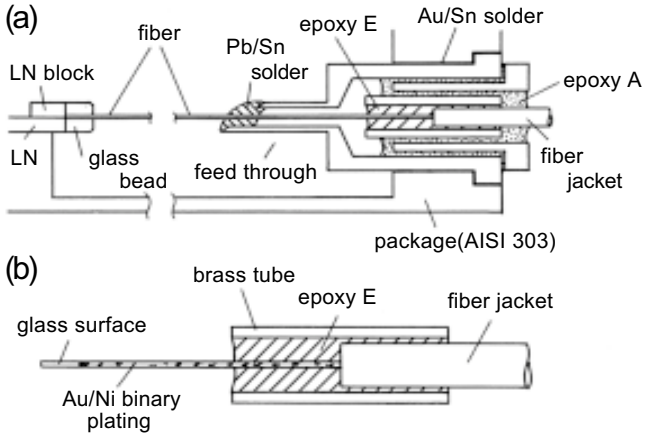

FIG. 1. Schematic illustration of the fiber feedthrough (a) and the installed fiber component (b), which were previously prepared before the assembly process.

scribed as "UV-400 fiber"). The fiber was further inserted into a commercial hytrel tube having an outer diameter of 900 μm for a protection of the UV-400 fiber surface. The length of the exposed fiber was about 35 mm (~3 mm inside of the brass tube), and the exposed fiber surface was previously metallized by a sequential electroless plating with nickel and gold except for the end of the fiber.

The fiber component of Fig.1b was fed into the fiber feedthrough of the packagem and after an optical axis alignment process with the LN waveguide chip, the exposed fiber was bonded to the LN chip by UV curable epoxy adhesive. The bonding strength was reinforced with an additional LN block and a glass bead, as shown in Fig.1a and Ref. [27]. After the bonding between the fiber and LN chip, the fiber was thrust 35 μm along the axis toward the LN chip and soldered at the end of the fiber feedthrough pipe, resulting in the fiber being bent slightly through the ~25-mm gap between the LN chip and the soldered point. The length of this intentional thrust was enough to cancel the opposite pulling movement of the fiber during the solder solidification process. When the tense fiber was soldered, the optical insertion loss of the device deteriorated (increase of several dB) due to the soldering. In the present procedure, namely the introduction of a slight bend in the fiber, almost no change of the optical insertion losses was observed as a result of the fiber bonding and soldering processes. Further, even after the soldering process, the same slight curve in the exposed fiber remained. If the pushed length of the fiber was not decreased by the soldering process, this bend in the fiber could cancel a fiber pulling caused by a large difference of thermal expansions of the fiber and the package. The fiber pulling length due to the package expansion as a result of a 50-K temperature increase, for instance, was calculated to be 22 μm for the present structure, while the previously pushed length was 35 μm. Actually, no deterioration was observed in the optical insertion losses of the devices after the heat cycle tests between -40 and 70°C, as described in Section 5.

After the fiber soldering process, a gap (~0.3 mm) between the inner space of the feedthrough and the brass tube of the fiber was filled with another brass tube and a room temperature curable epoxy adhesive A, as shown in Fig.1a. Finally, a rubber boot was bonded to cover the outside of the fiber feedthrough (not shown in Fig.1a). The UV-400 fiber and the hytrel loose tube were bonded together in the rubber boot. In the present feedthrough structure, a space inevitably remained around the fiber inside of the feedthrough because the adhesive material could hardly be injected through such a narrow space. The length of the space was about 5 mm along the metallized glass fiber. Such a cavity was not selected to improve the reliability of the exposed fiber because the fiber sometimes broke here due to a buckling deformation of the fiber. However, this problem was almost solved by a suitable choice of jacketed fiber and adhesive material for fiber fixing, as described in the next section. A buckling of the fiber, caused by the difference in thermal expansion of the materials, was estimated to be very small for the present ~5-mm gap structure and should not lead to a fiber break within an ordinary operation temperature of the device (see Section 4).

The above assembled to the package in dry N_2/He mixture (a dew point $\leq$ -40°C) [23].

3. CHOICE OF PROPERLY JACKETED OPTICAL FIBERS

In order to prevent the fiber breaks inside of the package fiber feedthrough, use of the UV-400 type fiber was necessary, especially for the devices being exposed to temperatures ranging from -40 to 70°C. Other fibers tightly coated with a hytrel or a polyvinyl chloride (PVC) were also acceptable for this purpose. However, fibers coated with inner silicone and outer nylon jackets were considered unsuitable for mechanically reliable LN devices. Such results were empirically known among device manufactures, but the nylon jacketed fibers are still used for device assembly, especially in Japan, perhaps because the jacket materials are easily removed [19, 20], etc. In this section, based on our experimental results, weaknesses of devices including the nylon-jacketed fibers were described.

Using the commercial nylon tight-jacketed fiber, LN modulator devices were fabricated via the assembly process mentioned in Section 2. After the assembly, 20 heat cycles between -20 and 70°C (ramp rate ≅2 K/min, soaking ≅30 min) and storage for 100 h at 80°C were sequentially carried out on the device to reject devices unfit for use. During this process, however, hereafter described as a "screening test," some devices failed due to

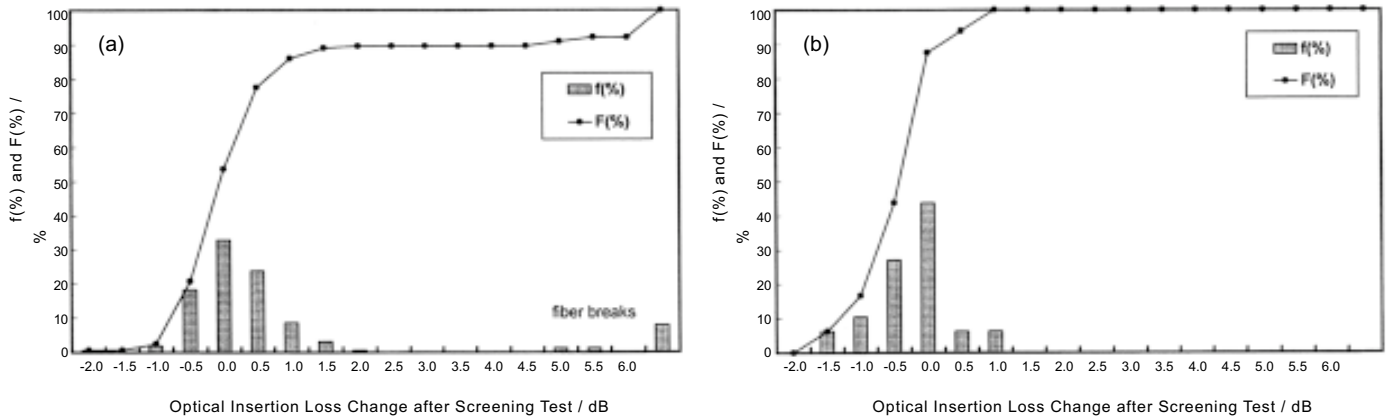

FIG. 2. A distribution f(%) and cumulative distribution F(%) of changes in optical insertion losses after the screening test. (a) The result for the devices assembled with nylon tightly jacketed fibers. (b) The present devices assembled using UV-400 fibers.

fiber breaks, as shown in Fig. 2a, where a distribution, f(%), and a cumulative distribution, F(%), of optical insertion loss changes after the screening test are presented for 164 fabricated modulator devices. The loss measurement was done with light of 1.5-μm wavelength, before and after the test. As seen, about 10% of the devices failed due to the fiber break. The fiber breaks were found to occur in the fiber feedthrough, as shown in Figs. 3a and 3b. Even the devices which had passed the screening test resulted in fiber breaks frequently during further environmental tests such as -40°C/70°C heat cycles: 6 in 10 devices failed during these 100 heat cycles. In the present devices with UV-400 fibers, however, the fiber breaks were successfully eliminated, as shown in Fig. 2b, in which the test result for 48 devices are plotted.

Fibers protruding from the jacket end and the resulting fiber buckling have been cited as reasons for fiber breaks in device packages [3]. This was sufficient reason to consider the conventional nylon jacketed fiber to be unuseable for practical devices. The frictional bonding strength between the glass fiber and the jacket material was measured for various kinds of fibers. In the measurement, the jacket materials were cut completely at first and the force needed to pull the jacket from the glass fiber was measured. As a result, the pulling force for the nylon jacketed fibers was 18-23 gf/mm on average for 10 each of three different manufacturer's fibers (standard deviation, S.D. = 3.5-6.1 gf/mm). However, other types of fiber exhibited larger pulling forces of 80 gf/mm (S.D. = 13 gf/mm) for UV-400 fibers, 86-104 gf/mm (S.D. = 23-28 gf/mm) for hytrel-jacketed fibers, and 172 gf/mm (S.D. = 48 gf/mm) for elastomer-jacketed fiber. The results indicated that because of the weaker bonding strength of the fiber/jacket interface in the nylon-jacketed fibers, the glass fiber stuck out when the jacket materials contracted due to a temperature change. Some nylon jacket material was found to deform rapidly due to a temperature change (40-80°C), judg-

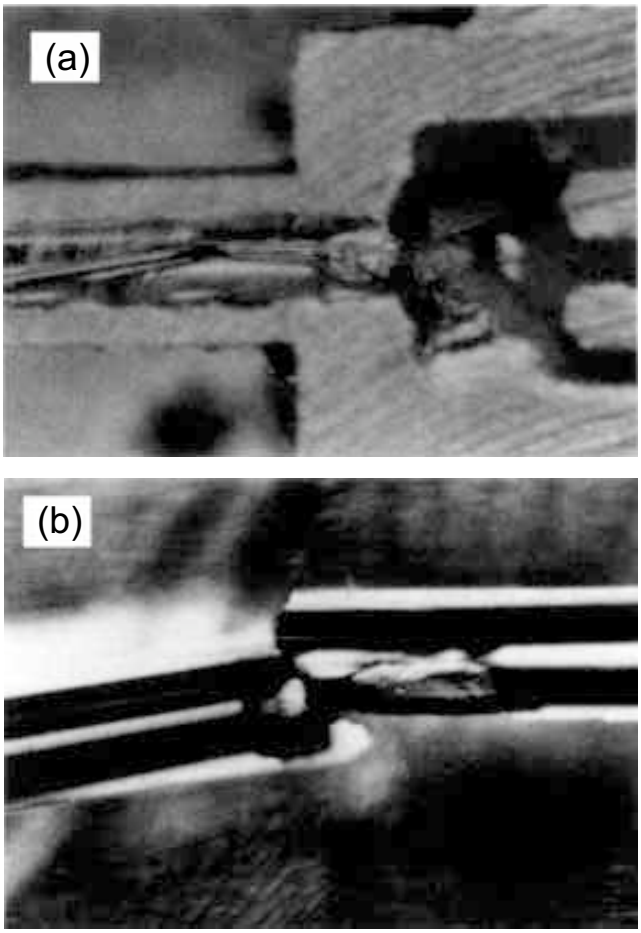

FIG. 3. Optical micrograph of the metallized fibers installed in the stainless steel feedthrough pipe. At the left end of the pipe, the fiber is fixed with solder while it is bonded with epoxy material at the other end (not shown in the photopraphs). (a) Example of a fiber break occuring in the pipe due to heat cycles. The break seems to originate from localized bending of the fiber due to fiber protruding from the jacket materials. (b) Extension of the fiber break of (a).

ing from observed changes in the curve of the nylon-jacketed fibers placed on a heater.

The fiber protruding phenomenon was further checked for the component shown in Fig. 1b under cyclic temperature changes. In this component, the movement of the fiber (and/or the jacket) could be suppressed by a bonding adhesive. As the heat cycles accumulated, however, the length of the protruding fiber which was bonded to the brass tube at the nylon jacket end increased. Table 1 exhibits exapmles of such protruding lengths of the fibers caused by 400 heat cycles between -20 and 70°C and by a subsequent 500 cycles between -40 and 70°C. Three kinds of fibers which were tightly jacketed with 0.9-mm outer diameter nylon, PVC, and 0.4-mm outer diameter UV-400 materials were investigated. The tube was bonded to the inserted exposed and jacketed fiber using a room temperature curable (A) or thermal curable (E) epoxy adhesive material [28, 29]. The results indicated that with an improper combination of the fiber jacket (nylon) and adhesive (A) materials, a fiber protrusion as long as 2 mm occurred within ordinary device operation and storage temperature ranges. This length was enough to buckle and to break the metallized fiber which was held within the short gap (5 mm in the present structure) [22]. Even in the combination of the nylon jacket and the stronger adhesive E, the protrusion length was larger than those of PVC and UV-400 fibers. Consequently, fibers such as UV-400 must be recommended for mechanically reliable devices.

4. ESTIMATION OF REDUCED FIBER BREAKS DUE TO HEAT CYCLES

By the use of properly jacketed fiber, fiber breaks in the feedthrough were almost eliminated. Here, the possibility of further breaks caused by a thermal expansion mismatch between the fiber and the package feedthrough is discussed. Figure 4 shows a schematic illustration of the present fiber feedthrough structure consisting of the exposed fiber, stainless steel pipe, and epoxy adhesive materials filled into one end of the pipe. The solder material at the other end of the pipe was excluded here because its thermal expansion was close to that of the stainless-steel pipe. The length of the pipe(L_p) was set to be 7 mm from the corresponding configuratin of the present structure. The bonding strength between the epoxy and the fiber was assumed to be strong enough so as not to be removed within an ordinary temperature range. Under the temperature change of ΔT, the following equations were obtained concerning the axial strains ($\in$) of this component:

$$(\in_f^T + \in_f^P) L_f + (\in_a^T + \in_a^P) L_a = (\in_p^T + \in_p^P) L_p \quad (1)$$

$$\in_f^T = \alpha_f^T \Delta T, \quad \in_a^T = \alpha_a^T \Delta T, \text{ and } \in_p^T = \alpha_p^T \Delta T \quad (2)$$

$$\in_f^P = P/(A_f E_f), \quad \in_a^P = P/(A_a E_a), \text{ and } \in_p^P = P/(A_p E_p). \quad (3)$$

Here, α, P, A, and E are the thermal expansion coefficient, the axial force applied to the fiber, the cross-sectional area, and Young's modulus of the materials, respectively. The subscripts denote fiber (f), adhesive material (a), and stainless steel pipe (p). The superscripts mean thermal-induced (T) and force-induced (P) strains $\in$. From Eqs. (1), (2), and (3), the relation of

$$P [L_p/(A_p E_p) - L_f/(A_f E_f) - L_a/(A_a E_a)] = \Delta T(\alpha_f L_f + \alpha_a L_a - \alpha_p L_p) \quad (4)$$

was derived. The values of P could be calculated, using parameters of Table 2, as ±42 gf for the epoxy adhesive material A and ±18 gf for epoxy E when ΔT= ±40°C. The sign of the P was positive for temperature decrease and

TABLE 1
Fiber Lengths (in mm) Protruding from the Fiber Jacket Ends Due to Heat-Cycle Application

Sample Configuration		400 cycles of -20/70℃			500 cycles of -40/70℃		
Jacket material	Adhesive	Min.	Max.	Average	Min.	Max.	Average
Nylon	A	1.62	2.35	2.140	—	—	2.574[a]
PVC	A	-0.01	0.01	0.004	-0.02	0.05	0.020
UV-acrylate	A	-0.04	0.08	0.014	-0.06	0.09	0.030
Nylon	E	0	0.04	0.020	0.03	0.07	0.050[b]
PVC	E	-0.01	0.03	0.006	-0.03	0.03	0.002
UV-acrylate	E	0	0.03	0.012	-0.03	0.04	0.004

Note. The samples consist of 50-cm-long jacketed fiber with 10 mm of jacket removed to expose the end of the fiber and 6-mm-long brass tube wihich is bonded by epoxy adhesive material at the boundary of the exposed and jacketed fiber. Each of the samples includes five speciments. The heat cycle tests are carried out first as 400 cycles between -20 and 70°C (ramp rate ~2°C/min), then as 500 cycles between -40 and 70°C (ramp rate ~10°C/min).

[a] Only one fiber specimen endured all heat cycles. Four other fibers failed as the primary coat appeared out from the brass tube about 18 mm.

[b] Only two fiber specimens remained without failure. In such failured specimens, the epoxy protruding from the brass tubes and the jacket stuck out a little from the tube.

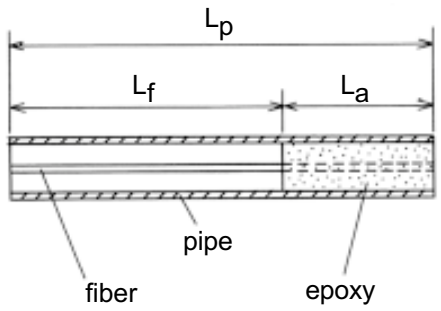

FIG. 4. Schematic illustration of the fiber feedthrough component. The length of the feedthrough pipe L_p is fixed here to be 7 mm. The exposed fiber is inserted into the pipe and bonded with epoxy adhesive material at the pipe end.

negative for temperature increase, indicating that the fiber was axially compressed when $\Delta T > 0$. Concerning tensile deformation of the fiber due to the cooling process, the estimated tensile force (few tons of gf) was two order of magnitudes smaller than the tensile strength of the exposed fiber and was not the reason for the fiber breaks. In the experiment, 500 gf of tensile force, 10 times the estimated value, was repetitively applied, more than 100 cycles, to three 5-mm-long exposed fibers, and no fiber breaks were observed.

Figures 5a, 5b, and 5c show schematically three kinds of fiber buckling caused by the axial compressive force. In the buckling shown in Fig. 5a, the critical force P for the buckling deformation is expressed by Euler's formula

$$P = E I \pi^2/4 L^2 , \quad (5)$$

where I is a moment of inertia of a cross section about the fiber axis and is calculated using a fiber diameter (D = 0.125 mm) from $I = \pi D^4/64$ [30]. When both ends of the fiber are fixed coaxially, as shown in Fig. 5b, the buckled fiber length is divided into four segments showing buckling similar to that in Fig. 5a, and by substitution of L in Eq. (5) with $L/4$, the P for buckling shown in Fig. 5b can be written as

$$P = 4 E I \pi^2/ L^2 . \quad (6)$$

Analogously, the equation for the buckling shown in Fig. 5c, where the fixed fiber ends are slightly offset, is obtained as

$$P = E I \pi^2/ L^2 . \quad (7)$$

In the assembled devices, the fibers were installed with a small offset in the fiber feedthrough because of the fiber alignment and an intentional fiber pushing processes (see Section 2). Therefore, the fiber buckling exhibited by Fig. 5c and Eq. (7) was discussed here. When the fiber length L was 4 to 5 mm, the critical force P for the buckling was calculated to be 35 to 40 gf. This value was comparable to the compressive force applied to the fiber under the ordinary heating process (Eq. (4)). As a result, during the operation of the devices, a slight fiber buckling occurs repetitively, possibly leading to a break in the fiber. In this regard, the influence of the repetitive buckling on the breaks in the exposed fibers was checked by the experiment.

The exposed fiber was hung between two brass ferrules, one of which was fixed on the substrate, the other being linked to a spring balance enabling it to slide along the fiber axis. The fiber was bonded to both ferrules with epoxy adhesive material, keeping the gap length of 5 mm. This 5-mm-long fiber was slightly and repetitively buckled by cyclical sliding of the ferrule, where the applied force was measured to be 20 to 50 gf. Three fibers were tested, two of which broke at almost the center of the fiber at 296 and 342 repetitions. The other fiber broke after 232 buckling cycles at the point close to the ferrule. The fractured face of the fibers was the same as that shown in Fig. 3b. The result suggests that the installed fibers might break if a repetitive slight buckling due to cyclic temperature change is applied.

Then, the possibility of preventing such cyclic buckling was considered. Figure 6 shows the critical lines beyond which the fiber buckling occurs, being calculated from Eqs. (4) and (7) as a function of temperature change ΔT and the exposed fiber length L in the 7-mm-long feedthrough pipe. The solid and broken lines correspond to the results for the use of epoxy adhesive materials E and A, respectively. The results of Fig. 6 are explained as follows. When the exposed fiber length is short, the exposed fiber experiences a greater compressive force due to

TABLE 2
Characteristic Parameters of the Materials Mentioned in Fig. 4 and Eq. (4)

	Optical fiber	Epoxy A	Epoxy E	Srainless steel pipe
α [°C^{-1}]	0.04×10^{-6}	67.0×10^{-6}	5.40×10^{-6}	16.4×10^{-6}
E [Pa]	7.31×10^{10}	$0.4\text{-}1.2 \times 10^{10}$	0.9×10^{10}	21.0×10^{10}
A [m^2]	1.23×10^{-8}	5.03×10^{-7}	5.03×10^{-7}	6.28×10^{-7}
L [m]	4.50×10^{-3}	2.50×10^{-3}	2.50×10^{-3}	7.00×10^{-3}

Note. α, E, A, and L denote thermal expansion coefficient, Youngí modulus, cross sectional area, and length, respectively. Diameters of the fiber, epoxy, and pipe are 0.125, 0.8, and 1.2 mm, respectively.

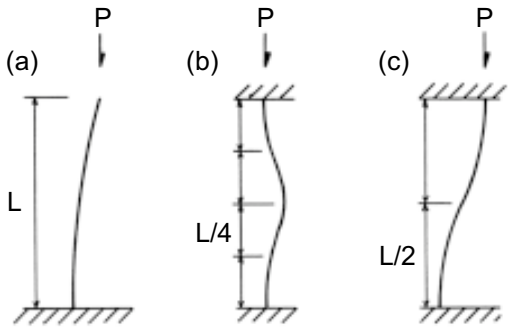

FIG. 5. Schematic illustrations of the buckling fibers. One end of the fiber is fixed and the other end is free (a), coaxially fixed (b), or off-axially fixed (c).

the larger thermal expansion of the long epoxy portion. On the other hand, as the exposed fiber length increases, the critical force P for the fiber buckling decreases by a power proportion to the square root of the exposed fiber length (see Eq. (7)). In Fig. 6, with an increase in the exposed fiber length from zero, the decreasing critical force P leads to the lower critical ΔT value. With a further increase in the exposed fiber length, however, the absolute expansion of the epoxy material reduces, resulting in an increase of the critical ΔT value. Then, the influence of the thermal expansion of the epoxy becomes negligibly small, but the contraction of the stainless steel pipe is the cause of the fiber buckling at negative ΔT.

In order to improve the temperature tolerance of the assembled fibers, the exposed length of the fiber must be as short as possible ($\ll$1 mm in the case of Fig. 6), as generally said. As seen in Fig. 6, however, a middle length of exposed fiber (~5 mm) gave also a high enough critical ΔT value. This result suggested that the present feedthrough structure of Fig. 1a, where an ~5-mm-long cavity was remaining, can almost eliminate the fiber breaks induced by heat cycles.

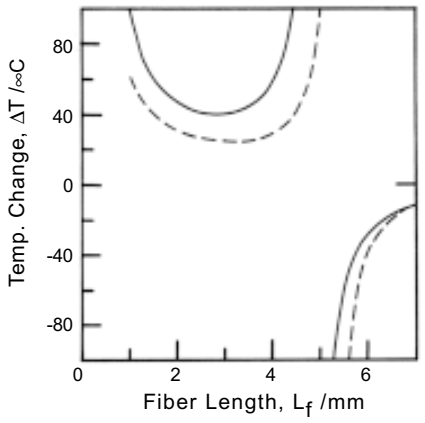

FIG. 6. The critical curves for occurrence of fiber buckling. The horizontal axis denotes the exposed fiber length L_f in Fig. 4, where the pipe length L_p is 7 mm. The vertical axis denotes the temperature change ΔT. The solid and broken curves are calculated for the feedthrough component using the adhesive materials E and A, respectively. A slight fiber buckling occurs in the region enclosed by the critical curves.

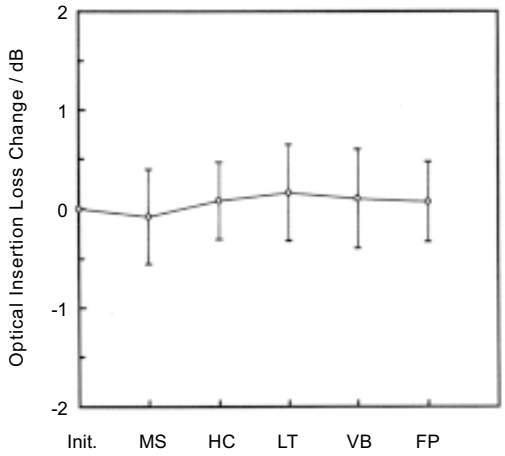

FIG. 7. Optical insertion loss changes measured for the 11 devices after 500-G mechanical shock (MS), -40/70°C heat cycle (HC), -50°C low temperature strorage (LT), 20-2000 Hz vibration (VB), and 1-kgf fiber pull (FP) tests. The error bars correspond to the standard deviation.

5. MECHANICAL TEST RESULTS

To assess a reduced fiber break in the proposed feedthrough structure, 13 LN Mach-Zehnder modulators assembled using the hytrel loose-tubed UV-400 fibers were exposed under various mechanical tests. The stainless steel package of the modulators were hermetically sealed under a dry N_2/He mixture by a seam welding technique. Most of the tests were the same with those in Bellcore's TR-NWT-000468. Namely, the following tests were carried out sequentially for 11 modulators, and the optical insertion losses of the samples were checked after each test.

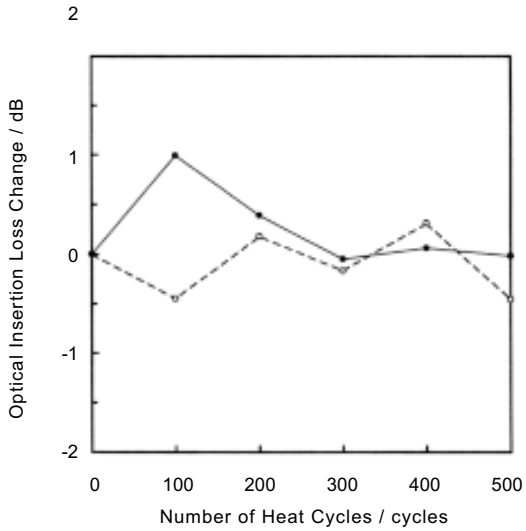

FIG. 8. Optical insertion loss changes of the two devices during 500 heat cycles between -40 and 70°C.

(1) mechanical shocks (MS): at 500 G peak acceleration with 0.5-1 ms pulse width, 5 times/axis;

(2) heat cycles (HC): between -40 and +70∞C, ~18 K/min ramp rate (measured in a test chamber), ~24 min soaking, 100 cycles;

(3) low temperature storage (LT): at -50∞C for 168 h;

(4) vibrations (VB): between 20 and 2000 Hz with 20 G acceleration, 4 min/cycle, 5 times/axis;

(5) fiber pull (FP): 1 kgf load for 10 s, 3 times/fiber.

Further, two other modulators were exposed under 500 heat cycles between -40 and 70◦C. The results are shown in Figs. 7 and 8 for the former and latter tests, respectively. Figure 7 is presented as average and standard deviation values for 11 samples. Throughout the tests, no fiber breaks were observed, and the change of optical insertion losses was quite small. Consequently, the proposed feedthrough structure was usable for the LN modulator packages with a high mechanical reliability.

6. CONCLUSIONS

The problem of optical fiber breaks in the stainless steel package for $LiNbO_3$ optical modulators was investigated. Although the present fiber feedthrough included a cavity in it, the fiber breaks due to fiber buckling in the cavity could be prevented, mainly by the use of proper optical fibers: the fiber coated with UV-cured acrylate material was used here in this regard. Several tens of devices have been fabricated actually without any fiber breaks, and no further breaks occurred even after Bellcore's TR-NWT-000468 mechanical tests for the similar samples. The possible fiber breaks problem in the hermetically sealed $LiNbO_3$ devices was almost solved by adoption of the present feedthrough structure. Further evaluation on the reliability of these packaged modulators is now in progress from the viewpoint of hermeticity and device performance stability.

ACKNOWLEDGEMENTS

The authors thank gratefully Mr. R. Kaizu, N. Miyamoto, and Dr. J. Minowa for useful discussions and Mr. Y. Niyama and T. Sugimoto for their help in the optical loss measurements.

REFERENCES

[1] W. W. Wood, "Long-term reliability of interconnection devices," in *OFC/IOOC'93 Technical Digest*, p.76, 1993.

[2] N. Yoshizawa, H. Tada, and Y. Katsuyama, "Strength improvement and fusion splicing for carbon-coated optical fiber," *J. Lightwave Technol.*, vol. 9, no. 4, 417 (1991).

[3] B. G. LeFerve, W. W. King, A. G. Carlisle, and K. B. Bradley, "Failure analysis of connector-terminated optical fibers: two case studies," *J. Lightwave Technol.*, vol. 11, no. 4, 537 (1993).

[4] W. R. Wagner, "Extrinsic fiber damage and its effect on the reliability of optical fiber connectors and splices," *SPIE Fiber Optic Components and Reliability*, vol. 1580, 168 (1991).

[5] B. G. LeFerve, "Reliability issues with connectors and splices," *SPIE Optical Materials Reliability and Testing*, vol. 1792, 39 (1992).

[6] B. G. LeFevre, "Failure mechanisms and reliability of fiber optic connectors and splices," *SPIE Fiber Optics Networks and Video Commun.*, vol. 1973, 264 (1993).

[7] G. Kiss, "Reliability of optical splices," *SPIE Fiber Optics Reliability and Testing*, vol. CR50, 118 (1993).

[8] B. G. LeFevre, "Reliability of passive optical components," *SPIE Fiber Optics Reliability and Testing*, vol. CR50, 105 (1993).

[9] N. Akasaka, T. Hattori, T. Nonaka, K. Oishi, and Y. Matsuda, "Design of optical fiber coating," in *Proc. of ACOFT'94*, pp. 375-378 (1994).

[10] G. S. Glaesemann, "Fiber reliability modeling for multiple stress-time histories," in *Proc. ACOFT'94*, pp. 341-346 (1994).

[11] T. T. Wang and H. M. Zupko, "Long-term mechanical behavior of optical fibers coated with a u.v.-curable epoxy acrylate," *J. Mater. Sci.*, vol. 13, 2241 (1978).

[12] M. J. Matthewson and C. R. kurkjian, "Strength measurement of optical fiber by bending," *J. Am.Ceram.Soc.*, vol. 69, no. 11, 815 (1986).

[13] V. V. Rondinella and M. J. Matthewson, "Coating additives for improved mechanical reliability of optical fiber," *J. Am. Ceram. Soc.*, vol. 77, no. 1, 73 (1994).

[14] T. A. Michalske, W. L. Smith, and B. C. Bunker, "Fatigue mechanisms in high-strength silica-glass fibers," *J. Am. Ceram. Soc.*, vol.74, no.8, 1993 (1991).

[15] D. Roberts, E. Cuellar, and L. Middleman, "Static fatigue of optical fibers in bending. II. Effect of humidity and proof stress on fatigue lifetimes," *SPIE Fiber Optics Reliability: Benign and Adverse Environments*, vol.842, 32 (1987).

[16] M. J. Matthewson, "Optical fiber reliability models," *SPIE Fiber Optics Reliability and Testing*, vol. CR50, 3 (1993).

[17] D. R. Biswas, "Optical fiber coatings," *SPIE Fiber Optics Reliability and Testing*, vol. CR50, 63 (1993).

[18] D. K. Paul, "Critical issues in assuring long lifetime and fail-safe operation of optical communications network," *SPIE Fiber Optics Reliability and Testing*, vol. CR50, 232 (1993).

[19] H. Nagata, N. Miyamoto, and R. Kaizu, "Highly reliable jacket cutter for optical fibers," *IEICE Trans. Fundamentals in Electron. Commun. and Comput. Sci.*, vol. E76-A, no. 7, 1263 (1993).

[20] H. Nagata, N. Miyamoto, T. Saito, and R. Kaizu, "Reliable jacket stripping of optical fibers," *J. Lightwave Technol.*, vol. 12, no. 5, 727 (1994).

[21] Y. Yamazaki, Y. Ejiri, K. Furusawa, O. Harada, H. Nakashima, I. Sakurai, and M. Kondoh, "Fiber seal design for OS-280M optical fiber submarine repeater," in *Proc. of SUBOPTIC'86*, pp.219-224 (1986).

[22] N. Mitsugi, H. Nagata, M. Shiroishi, N. Miyamoto, and R. Kaizu, "Optical fiber breaks due to buckling: problems in device packaging," *Opt. Fiber Technol.* vol. 1, 278 (1995).

[23] H. Nagata and J. Ichikawa, "Progress and problems in reliability of Ti:$LiNbO_3$ optical intensity modulators," *Opt. Engineering* vol. 34, no. 11 (1995).

[24] for example, R. R. Tummala and E. J. Rymaszewski, "Micro-electronics packaging handbook," Van Nostrand Reinhold, New York, 1989.

[25] H. Nagata, M. Yamada, T. Sugamata, M. Shiroishi, H. Honda, M. Sakuma, Y. Miyama, T. Noguchi, N. Mitsugi, and J. Ogiwara, "Reliability evaluation of hermetically sealed Ti:$LiNbO_3$ optical modulators," in *Proc. of 21st Eur. Conf. on Opt. Comm*. (*ECOC '95, Brussels*), pp.905-908 (1995).

[26] private communication from Mr. M. Yamada of Sumitomo Osaka Cement Co., Ltd.

[27] H. Nagata, M. Shiroishi, Y. Miyama, N. Mitsugi, and N. Miyamoto, "Evaluation of new uv-curable adhesive material for stable bonding between optical fibers and waveguide devices: problems in device packaging," *Opt. Fiber Technol.* vol. 1, 283 (1995).

[28] CIBA-GEIGY Japan Co., ARALDITE Adhesive (parameters in Table 2 are for ARALDITE AV138 and HV998).

[29] EPO-TEK CO., EPO-TEK 353ND Adhesive.

[30] E. Suhir, in *Structural Analysis in Microelectronic and Fiber-Optic Systems*: vol. I, "Fundamentals of structural analysis," Part 2, Van Nostrand Reinhold, New York, 1991.